NRC Research and/or Technical Assistance Rept

PDR

EGG-NSMD-6155

February 1983

FRAP-T6 ANALYSIS OF PELLET CLADDING MECHANICAL INTERACTION

V. N. Shah

Idaho National Engineering Laboratory

Operated by the U.S. Department of Energy

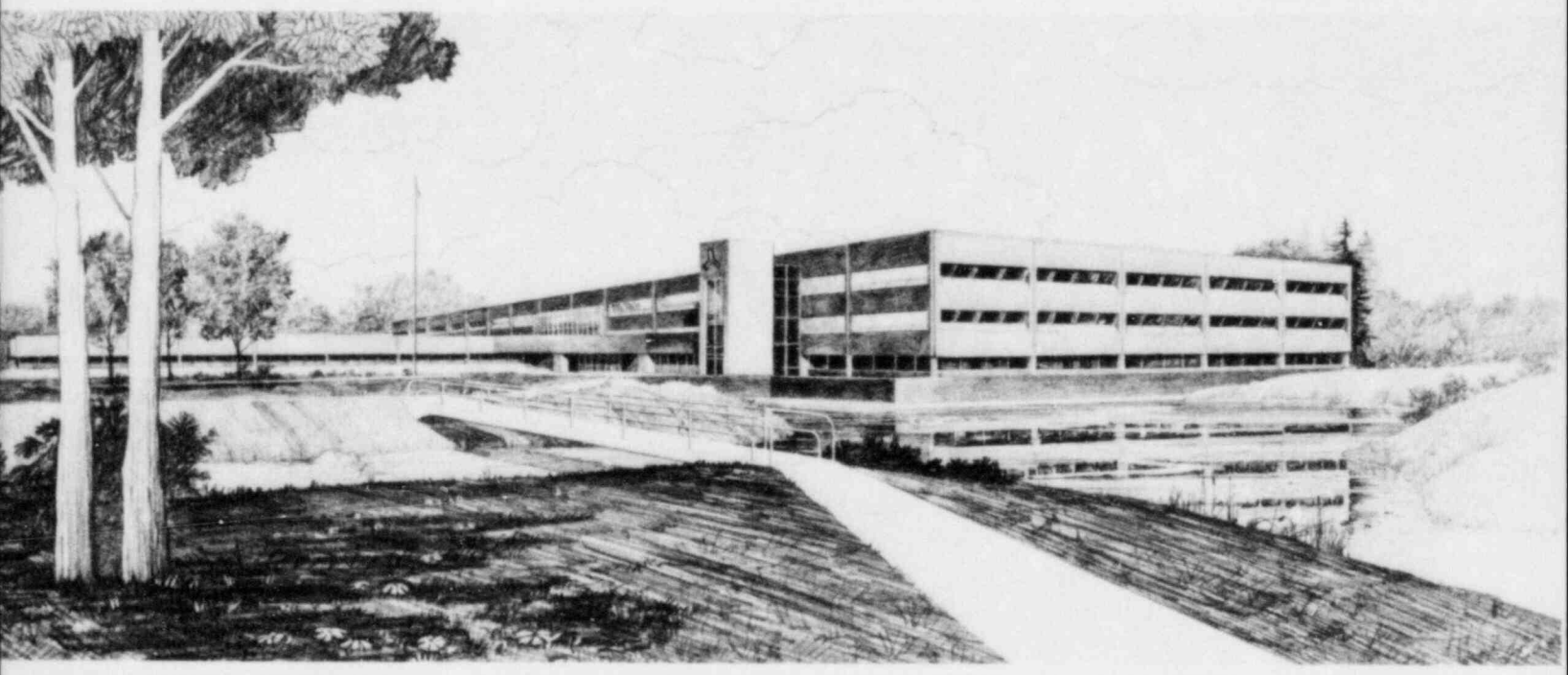

This is an informal report intended for use as a preliminary or working document

Prepared for the

U.S. NUCLEAR REGULATORY COMMISSION

Under DOE Contract No. DE-AC07-73ID01570

Fin. No. A6050

EG&G Idaho

EG&G Idaho, Inc.

FORM EG&G-398
(Rev. 03-82)

INTERIM REPORT

Accession No. _____

Report No. EGG-NSMD-6155

Contract Program or Project Title: Fuel Behavior Development Program

Subject of this Document: FRAP-T6 Analysis of Pellet Cladding Mechanical Interaction

Type of Document: Informal Technical Report

Author(s): V. N. Shah

Date of Document: February 1983

Responsible NRC Individual and NRC Office or Division: G. P. Marino, NRC-RES

EG&G Idaho, Inc.
Idaho Falls, Idaho **83415**

Prepared for the
U.S. Nuclear Regulatory Commission
Washington, D.C.
Under DOE Contract No. **DE-AC07-76ID01570**
NRC FIN No. A6050

INTERIM REPORT

ABSTRACT

This report presents comparisons between FRAP-T6 calculations of the mechanical resonse of fuel rods and corresponding test results for conditions involving pellet-cladding mechanical interaction. For these calculations, FRAP-T6 was modified to include a newly developed fuel compliance model and a revised cladding strength model. The mechanical response of the fuel rods consists of the cladding axial elongation, cladding hoop strain, and the fuel centerline temperature. The test results are from Halden fuel rod irradiation experiments IFA-508, IFA-509, and IFA-512 at low and moderate fuel burnup.

The comparisons presented in this report show good agreement between the modified FRAP-T6 calculations of cladding strains and the corresponding measured strains. These comparisons also show that addition of a fuel compliance model significantly improves the accuracy of calculations of cladding hoop strain. The revised cladding strength model improves the accuracy of calculated cladding permanent strain. Accurate calculations of cladding strains (and therefore, cladding stresses) are required to determine if fuel cladding will fail as a result of pellet-cladding mechanical interaction.

SUMMARY

This report presents comparisons of FRAP-T6 calculations of the mechanical response of fuel rods and corresponding test results for conditions involving PCMI. The test results are for five fuel rods from three well characterized Halden irradiation experiments. An empirical model of fuel compliance, which is needed to calculate maximum cladding hoop stress, has been developed for FRAP-T6 and is presented in this report. A material property routine in MATPRO is modified to correct the calculation of cladding yield and ultimate strengths. These modifications are also described in this report.

Comparisons between the FRAP-T6 calculations and corresponding experimental measurements show that the development of the compliance model and strength modifications have significantly improved the accuracy of the FRAP-T6 calculations of the cladding stresses. This conclusion is supported by the comparisons between the calculated and measured cladding axial strains, permanent axial strains and maximum hoop strains. Several recommendations are made for further improvement of the structural models in FRAP-T6 to improve the accuracy of cladding stress calculations to a degree acceptable for reliably determining fuel rod failure probabilities for commercial rods due to stress corrosion cracking.

ACKNOWLEDGEMENT

The author thanks D. Lanning of the Pacific Northwest Laboratory for providing FRAPCON-2 input decks and G. A. Berna for performing FRAPCON-2 analyses. The author expresses his thanks for guidance received from several individuals in preparing the FRAP-T6 code input: E. T. Laats for radial power profile inputs, L. J. Siefken for overall FRAP-T6 inputs, and D. L. Hagrman for helping to modify the cladding strength models.

CONTENTS

FIGURES

TABLE

FRAP-T6 ANALYSIS OF PELLET CLADDING MECHANICAL INTERACTION

V. N. Shah

1. INTRODUCTION

During transient reactor events in which significant departure from nucleate boiling does not occur, some of the fuel rods may fail due to crack initiation and propagation induced by mechanical interactions between the fuel pellets and caldding. These processes may also be enhanced by fission-product assisted stress-corrosion cracking (SCC). Cladding failure is significant because it results in the release of fission products from the fuel rods to the reactor coolant. One goal of the FRAP-T6 code maintenance/improvement task is to provide a capability for calculating the probability of cladding failure due to pellet-cladding mechanical interaction (PCMI) and SCC.

Factors affecting the initiation of cladding cracks and crack propagation are fuel rod thermal response, cladding stresses, fuel rod internal fission product environment, cladding materials properties, and fuel rod irradiation history. FRAP-T6 has the models required to characterize the thermal response of a fuel rod during transients, and these models have been assessed.[1,2] The mechanics subcode (FRACAS-II) in FRAP-T6 includes most of the models needed to calculate cladding stresses.[3,4,5] As will be discussed, some additional embellishments of the models are needed to complete the stress analysis capability. FRAP-T6 has two fission gas release models: FASTGRASS[6], which was developed by Argonne National Laboratory, and a MATPRO model called CESOID.[7] Recently, a SCC model developed by EPRI has been incorporated in FRAP-T6.[8] This model calculates crack propagation taking into account the irradiation hardening of the cladding and has significantly improved the failure calculations of FRAP-T6 for fuel rods experiencing PCMI and with fuel burnup greater than 11.5 GWd/tUO_2. If a model of fuel rod gap gas release to coolant, such as the FGRELG model[9] developed for the SCDAP code, were added to FRAP-T6, FRAP-T6 would represent a basic capability for analyzing PCMI-SCC cladding failures and the extent of fission product release from the failed cladding.

There are three cladding stress components that must be considered in a PCMI-SCC analysis: uniform axial stress due to axial PCMI, maximum hoop stress due to radial PCMI at pellet-pellet interfaces, and localized axial stress caused by formation of circumferential ridges at pellet-pellet interfaces during radial PCMI.[10] During 1982, models were developed for the FRACAS-II subcode of FRAP-T6 to calculate uniform axial stress.[4,5] A model of fuel compliance, which is needed to calculate maximum cladding hoop stress, has also been developed for FRAP-T6. This model is described in this report. FRACAS-II does not include a model for calculating localized axial stress. As FRAP-T6 is designed to analyze a whole fuel rod, an empirical model rather than a mechanistic model is more suitable for calculating localized axial stress due to ridge formation.

This report presents comparisons of FRAP-T6 calculations of the mechanical response of fuel rods and corresponding test results for conditions involving PCMI. The test results are for five fuel rods from three well characterized Halden irradiation experiments. The five fuel rods are Rods 11 and 32 from IFA-508,[11] Rods B1 and B2 from IFA-509,[12] and Rod C from IFA-512.[13] The last three rods were included in a workshop on modeling reactor fuel performance organized by the Halden Porgram Group during June 1982.[14]

For the FRAP-T6 calculations of the test fuel rods, FRAP-T6 was modified to include the fuel compliance model mentioned above and a revised cladding strengtn model. Early calculations of the test rods indicated that FRAP-T6 would not adequately calculate cladding hoop stress unless fuel compliance was considered by FRACAS-II. Therefore, a compliance model was developed and incorporated in FRAP-T6 for the calculations and comparisons presented in this report. The approach used to implement the model in FRAP-T6 was selected to allow the facility of the compliance model to be demonstrated within the time provided for this task. As discussed in this report it is not the desired approach and, thus, is considered only as a temporary FRAP-T6 update. The revisions to the cladding strength model were required because the existing model provided values of yield strength and ultimate strength that were not appropriate for the Halden fuel rod cladding. These revisions are described in this report.

Section 2 presents a description of the fuel compliance model and the approach used to implement the model in FRAP-T6 on a temporary basis. The desired approach for permanent installation of the model is discussed in Appendix A. Section 3 presents the comparisons between the FRAP-T6 calculations and the measured cladding strains and fuel centerline temperatures. Section 4 presents conclusions and recommendations for other model improvements needed to complete the FRAP-T6 PCMI-SCC analysis capability.

2. DESCRIPTION OF FUEL COMPLIANCE MODEL

FRAP-T6 overpredicts cladding hoop strains during PCMI as demonstrated by comparison with experimental data for IFA-508, Rod 11 (See Figure 1). The calculated maximum cladding hoop strain is 3.5 times greater than the corresponding measured data. This overprediction of cladding hoop strains results from an inadequate representation of cracked fuel compliance in the FRAP-T6 code. To remove this deficiency, a compliance model was developed for the FRAP-T6 code. This model is based on the hoop strain data for IFA-508, Rod 11 and is described in this section. The FRAP-T6 code with the compliance model (and cladding strength modifications to be described) is hereafter referred to as the modified FRAP-T6 code.

The thermal and mechanical behavior of fuel rods is significantly influenced by the relocation and compliance of cracked fuel pellets. The outward movement of the pellet fragments results in structurally softer pellets with crack voids which accommodate some fraction of the thermoelastic pellet deformation and make the pellet more compliant under the restraint of the cladding during PCMI. It is difficult to model pellet compliance mechanistically because of the random nature of the pellet cracking. Therefore, modeling of the pellet compliance is best treated empirically.

The material properties of the fuel may be modified to model pellet compliance. Using this approach, Ito et al.,[15] modeled pellet compliance by reducing the modulus of elasticity, E, or the thermal expansion coefficient, α, of the cracked fuel. Ito found that the modification of E was more promising than the modification of α for describing compliance of a cracked and relocated pellet. A compliance model based on a modified E was developed and incorporated in FRAP-T6, but was found unacceptable for two reasons:

1. A large reduction in E was not sufficient to reduce the calculated maximum cladding hoop strain to a magnitude corresponding with the measurement in IFA-508, Rod 11. For IFA-508, Rod 11, a 99.5% reduction in the modulus of fuel

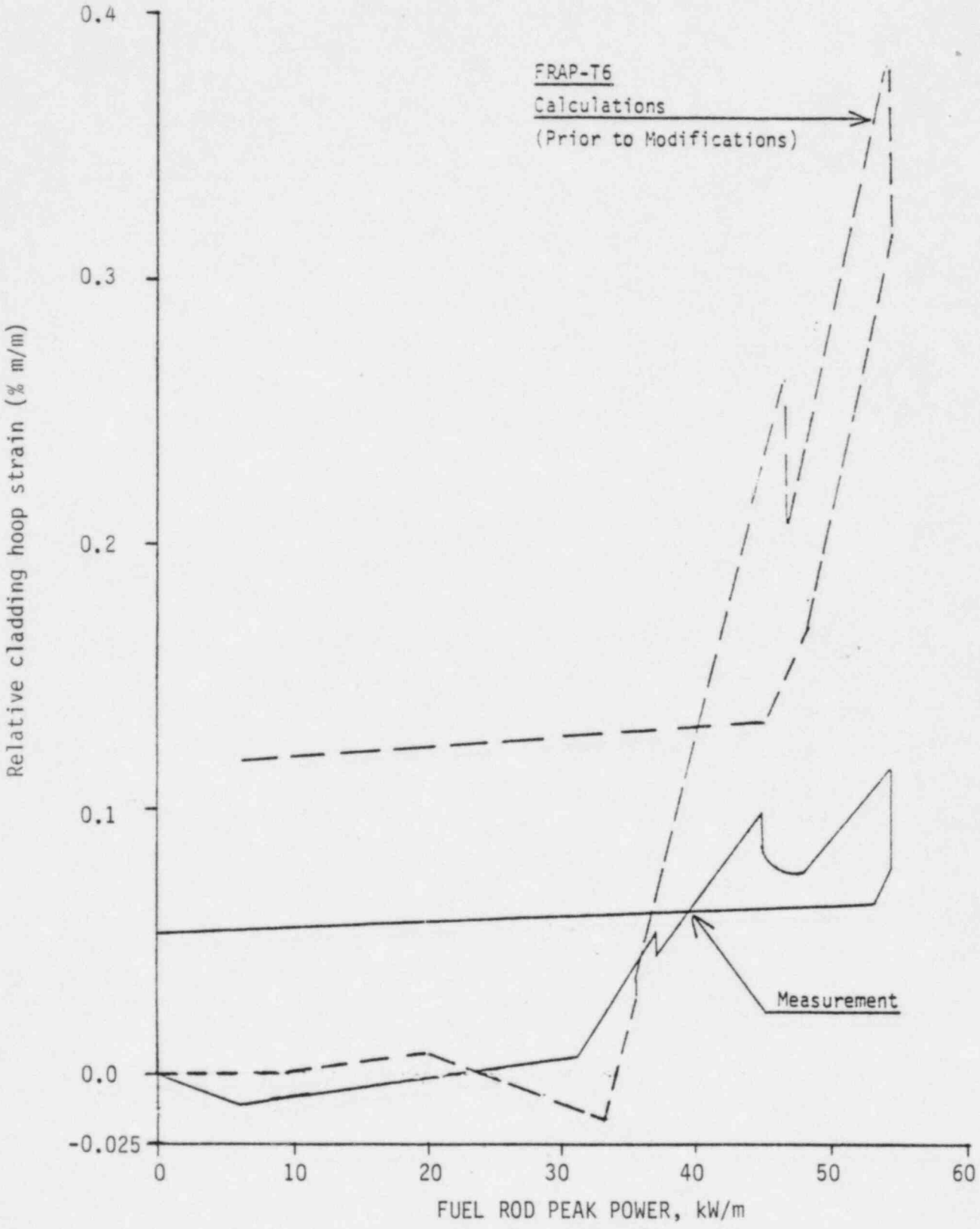

Figure 1. Calculated and measured cladding hoop strains versus power for IFA-508 Rod 11 using FRAP-T6 prior to current modifications.

elasticity reduced the maximum calculated cladding hoop strain from 0.38% to 0.21%, while the corresponding measured hoop strain is 0.115%.

2. A reduction of E introduced numerical instability in the FRAP-T6 calculations.

Pellet compliance represents a reduction of the inplane structural stiffness of the pellet which is due to geometrical changes in the pellet and not due to changes in the material properties. Therefore, a compliance model based on modification of material properties is an indirect and an artificial approach. A direct approach representing the overall inplane geometrical changes in the pellet was developed for FRAP-T6. A similar direct approach was successfully implemented in FRAP-T6 to represent effective thermal expansion of fuel.[4]

The FRAP-T6 fuel compliance model imposes a fraction of the pellet expansion on the cladding during PCMI. The inplane expansion of the pellet is multiplied by a compliance factor and is then imposed on the cladding. Based on the IFA-508, Rod 11 measured cladding hoop strains, a compliance factor of 0.25 is found suitable. This model reduces the maximum cladding hoop strain from 0.35% to 0.165%, while the corresponding measured maximum hoop strain is 0.115%. The remaining difference between the calculated and measured hoop strain may be reduced by modifying the fuel relocation relaxation and fuel creep models in the FRAP-T6 code. This is supported by the discussion in Section 4.

The fuel compliance model is implemented in FRAP-T6 in the following manner. In function GAPTX, the fuel-cladding gap is calculated with the following equation:

$$GAPTX = URC - (URF - DELTA)\ COMPF \qquad (1)$$

where

GAPTX = gap between cladding and fuel (m)

URC = radial displacement of cladding inside surface (m)

URF = radial displacement of fuel outside surface (m)

DELTA = as-fabricated fuel-cladding gap (m)

COMPF = compliance factor

= 0.25.

A compliance factor of 1.0 implies that effects of pellet cracks are ignored. In subroutine TRANSF, the following relation is used to impose only a portion of the fuel radial expansion on the cladding during radial PCMI (GAPTX is zero or negative):

$$URC = (URF - DELTA)\ COMPF. \tag{2}$$

Equation (2) is incorporated in the transfer matrix for radial mechanical interaction between pellet and cladding. Equation (1) increases the size of the radial gap between the pellet and the cladding. To initiate radial PCMI for Rod 11 at about the same power as observed in the experiment (see Figure 2), the fuel relocation model is modified by changing the coefficient of the linear heat rate term, P, from 0.01 to 0.04. The modified fuel relocation model is

$$R_e = G_o\,[0.4 + (0.04P - 0.3)\,e^{aBu}]$$

$$+ (0.6G_o - A)(1 - e^{bBu}) \tag{3}$$

where

R_e = relocation (m)

G_o = initial fuel-cladding gap (m)

P = linear heat rate (kW/m)

Bu = burnup (MWs/kgU)

a,b,A = experimental constants.

Also, the locking gap is changed from 0.0008 to 0.0002 m.

The purpose of implementing the compliance model in FRAP-T6 as described above was to assess whether or not this model would improve calculations of cladding hoop strains during PCMI conditions. As such, the implementation used is crude and only of a temporary nature. Part of this implementation approach, Equation (1), is not desirable because it requires modification of the fuel relocation model and locking gap parameter. It is prefered that the implementation of the pellet compliance model not require any additional changes in the fuel relocation model and the locking gap parameter. In addition, Equation (1) causes initiation of radial PCMI in small gap rods with relatively high fuel burnup at the beginning of a power cycle (see Figures 4, 9, and 10). Because the compliance model does improve the calculation of cladding hoop strains, it is recommended that the model be permanently implemented in FRAP-T6 but the implementation be modified so that the additional changes of the relocation model and locking gap parameter are not required. The proposed implementation of the fuel compliance model is described in Appendix A.

3. FUEL PERFORMANCE MODELING

Five fuel rods from three different Halden tests were analyzed with FRAP-T6 to evaluate the code's capabilities to model the mechanical behavior of fuel. Two rods, Rod 11 and Rod 32, are from IFA-508, two rods (Rod B1 and Rod B2) are from IFA-509, and one rod (Rod C) is from IFA-512. Rod 11 was tested at beginning-of-life, while the other rods were tested at a fuel burnup ranging from 3 GWd/tUO_2 to 15 GWd/tUO_2. The cladding hoop strains, cladding axial strains, and the fuel centerline temperatures calculated with FRAP-T6 are compared with the corresponding test results. The modified FRAP-T6 calculational results presented in this section included the compliance model discussed in Section 2. The temporary implementation scheme for this model, also discussed in Section 2, was used.

3.1 IFA-508 Experiment

The compliance model is based on the measured cladding hoop strain data of Rod 11 in the IFA-508 experiment. Therefore, the FRAP-T6 calculations for Rod 11 are presented first. The physical dimensions and material properties of Rods 11 and 32 are identical,[11] but data from Rod 11 are shown for beginning-of-life while data from Rod 32 are shown for 12.5 GWd/tUO_2. FRAP-T6 calculations for Rod 32 are presented here to assess the application of the compliance model at relatively high burnup.

3.1.1 Analysis of Rod 11

The physical dimensions, material properties, axial power profile, and power cycle for IFA-508, Rod 11 were reported during the developmental assessment of FRACAS-II.[16]

Early calculational results indicated that the FRAP-T6 calculations of cladding yield strength and ultimate strength were greater than the corresponding measurements. The FRAP-T6 calculations were 343.4 and 412.4 MPa, respectively, for the yield strength and ultimate strength at 616 K, while the corresponding measurements are 140 and 240 MPa, respectively. To correct this deficiency, the material property routine

CKMN in the MATPRO[7] subcode was modified. The modifications in CKMN consist of multiplying the strength coefficient by the factor 0.67 and the strain hardening exponent by the factor 1.75. These modifications reduce the yield strength to 138.8 MPa and the ultimate strength to 239.71 MPa. The various cladding yield and ultimate strengths are summarized in Table 1. Reducing the yield strength causes increased permanent cladding strains during PCMI.

TABLE 1. COMPARISON OF CLADDING STRENGTHS AT 616 K FOR IFA-508, ROD 11

	FRAP-T6		
Strength (MPa)	No Modifications	Modified CKMN	IFA-508 Test
Yield	343.4	138.8	140
Ultimate	412.4	239.7	240

Figure 2 shows a comparison of calculated and measured relative cladding extension for Rod 11 versus fuel rod peak power. Two sets of calculations are compared with the experimental data: FRAP-T6 calculations prior to addition of the compliance model and strength modifications and FRAP-T6 calculations after addition of the compliance model and strength modifications. The FRAP-T6 code with the compliance model and strength reductions is referred to as modified FRAP-T6. The following observations are made:

1. At maximum power, the FRAP-T6 calculation of relative cladding extension is 13% less than the corresponding measurement and the modified FRAP-T6 calculation of relative cladding extension is 6% greater than the corresponding measurement. As expected, the compliance model does not significantly affect the magnitude of the calculated maximum cladding axial strain.

2. The modified FRAP-T6 calculations show relaxation of the cladding axial extension when power is held constant: 0.035 mm at 36 kW/m, 0.05 mm at 47 kW/m and 0.2 mm at 54 kW/m. The

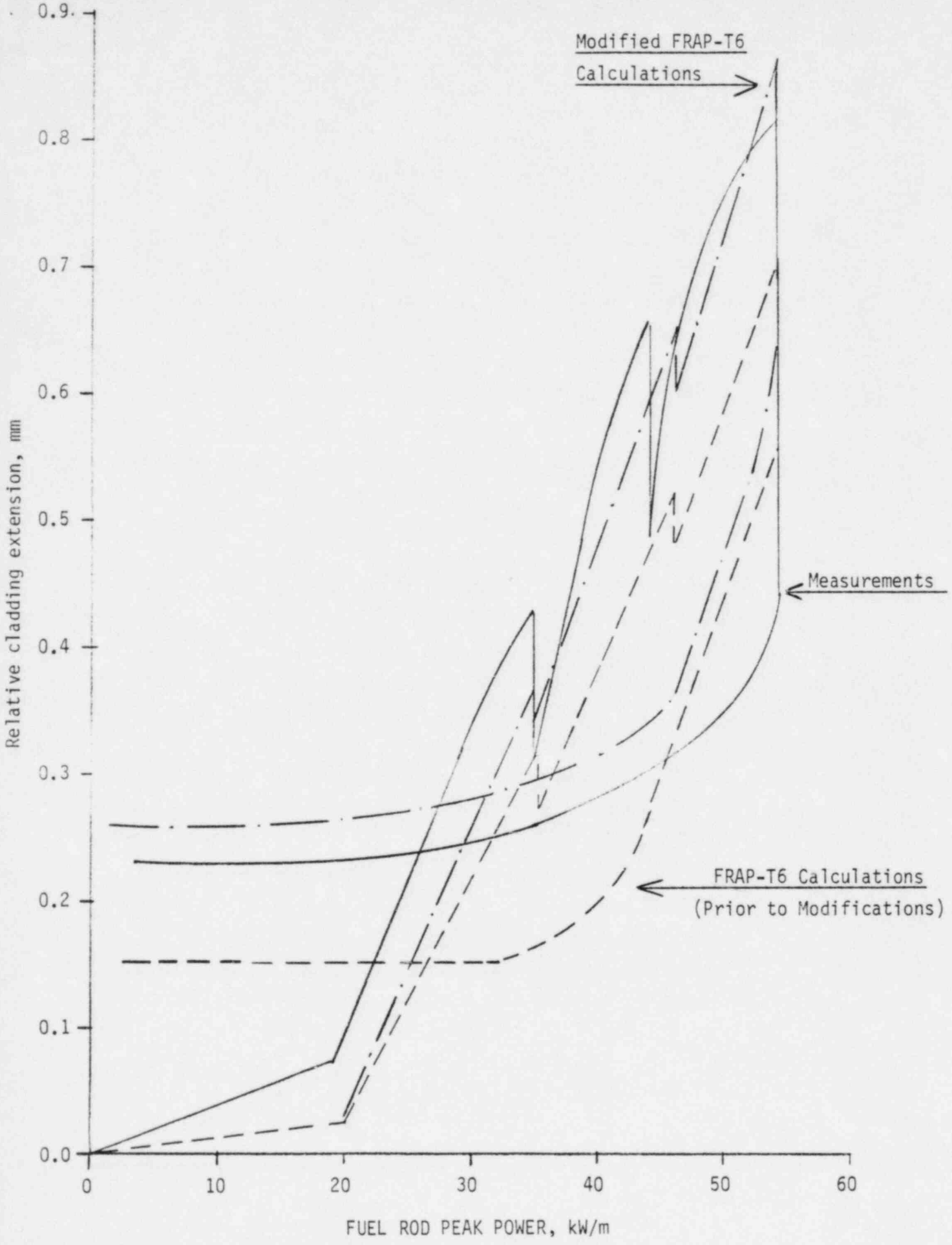

Figure 2. Calculated and measured cladding axial extension versus power for IFA-508 Rod 11 showing FRAP-T6 calculations before and after modifications.

corresponding measurements are 0.125 mm, 0.175 mm and 0.38 mm, respectively. Relaxation in cladding extension is due to fuel creep. Therefore, the significant difference between the modified FRAP-T6 calculations and measured cladding axial relaxation implies a deficiency in the fuel creep model.

3. The modified FRAP-T6 code calculates 0.065% for the permanent axial strain at the end of the power cycle while the corresponding measurement is 0.059%. The modified FRAP-T6 without strength reduction calculates 0.005% for the permanent axial strain. Therefore, the appropriate reductions in cladding strengths have resulted in significantly better agreement between the modified FRAP-T6 calculations and the measurements of permanent axial strain.

4. At the beginning of the power cycle in the range of 0 to 20 kW/m, the modified FRAP-T6 calculations of cladding axial extension correspond to cladding thermal expansion in the axial direction. In this low range of power, test results for cladding axial extension are greater than the corresponding modified FRAP-T6 calculations which implies that a soft axial PCMI is taking place. The existance of axial PCMI is confirmed by the negative hoop strain shown in Figure 3.

5. One observation that is not apparent in Figure 2 is that fuel creep causes tensile residual stresses near the center of the fuel during a power reduction. This may cause fuel cracking. The formation of cracks in the central portion of the fuel during a power reduction was reported in the postirradiation examination results for the irradiation effects Test IE-3[17]

Figure 3 shows a comparison of calculated and measured relative cladding hoop strains for Rod 11 versus average fuel rod peak power. Two sets of calculations are shown along with the experimental data: FRAP-T6

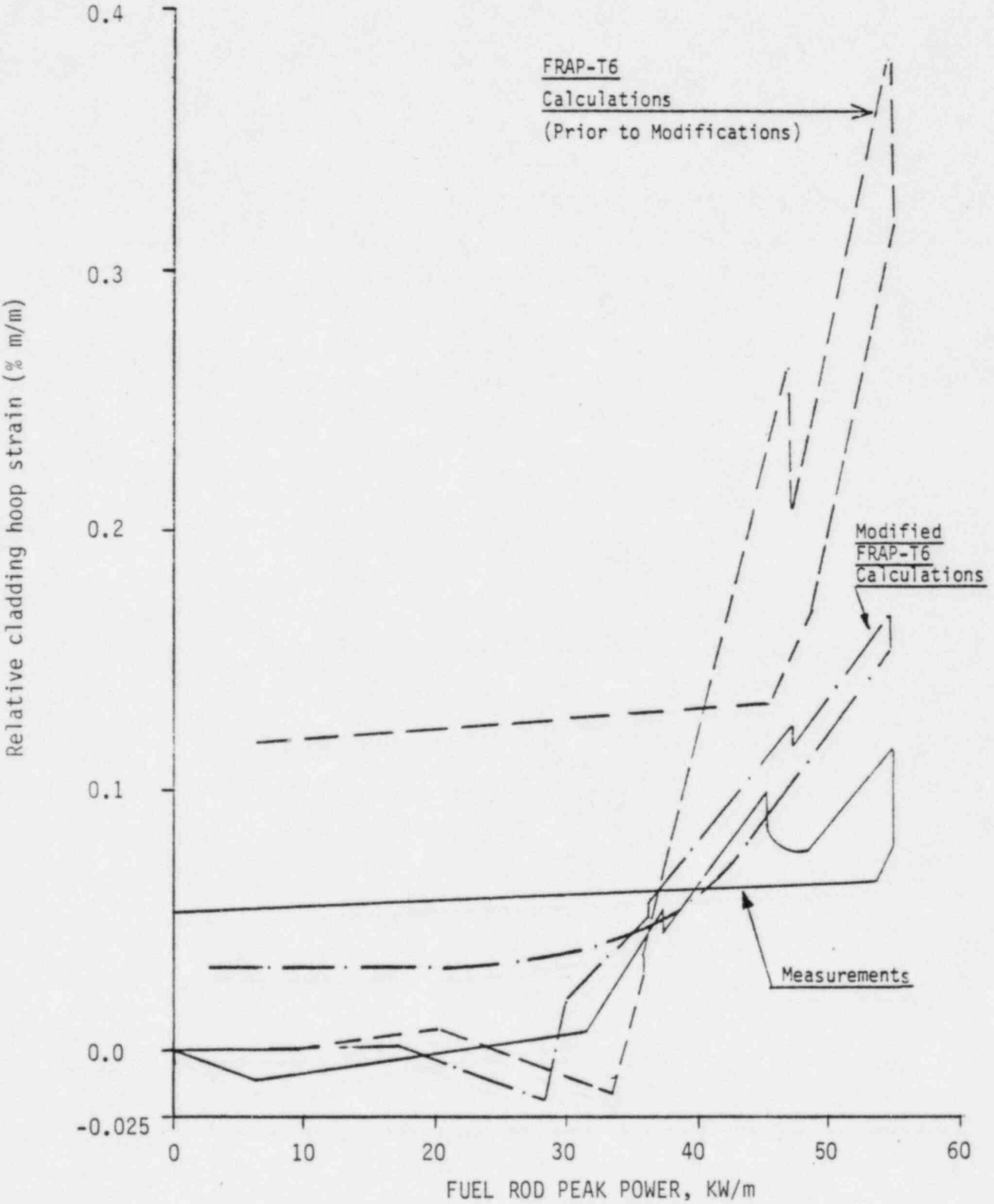

Figure 3. Calculated and measured cladding hoop strains versus power for IFA-508 Rod 11 using FRAP-T6 before and after modifications.

calculations prior to addition of the compliance model and strength modifications and the modified FRAP-T6 calculations. The following observations are made:

1. Comparison of the FRAP-T6 calculation with the measured cladding hoop strain shows that the difference between the cladding hoop strains increases as power increases. At maximum power the FRAP-T6 calculation of relative cladding hoop strain is 230% greater than the corresponding measurements. Comparison of the modified FRAP-T6 calculation with the measured cladding hoop strain shows that the difference between the cladding hoop strains is less than the corresponding difference between the FRAP-T6 calculation and the test measurement. At maximum power, the modified FRAP-T6 calculation of relative cladding hoop strain is 45% greater than the corresponding measurement.

2. At maximum power, the modified FRAP-T6 calculation of the relaxation of cladding hoop strain is 60% smaller than the corresponding measurement. When power was held constant at 36 kW/m, the modified FRAP-T6 calculations show that the cladding hoop strain is increased by 0.005% while the corresponding measurements show that the cladding hoop strain is decreased by 0.01%. Changes in the cladding hoop strain during PCMI while holding power constant are due to relaxation of the fuel relocation. Therefore, modifications in the fuel relocation relaxation model are needed to reduce the discrepancies between the modified FRAP-T6 calculations and the experimental measurements.

The comparisons presented above indicate that the addition of the compliance model has significantly improved the cladding hoop strain calculations when using FRAP-T6 with FRACAS-II. As expected, the comparisons also indicate that the addition of the compliance model has little effect on the FRAP-T6 calculations of cladding axial extension. In addition, the above comparisons show that the modifications of yield and

ultimate strength have significantly improved the permanent cladding strain calculations. These modified cladding strengths (yield and ultimate) are used in the remaining analyses.

3.1.2 Analysis of Rod 32

The physical dimensions, material properties, and axial power profile for Rod 32 are identical to those for Rod 11. Rod 32 was irradiated at extended low power to the burnup of 12.5 GWd/tUO_2 and was then subjected to a power cycle similar to the one used for Rod 11.

FRAP-T6 analysis of an irradiated fuel rod requires that certain modeling guidelines are followed. These guidelines are described first, and then the FRAP-T6 calculations for Rod 32 are presented.

During extended low power irradiation, fuel deformation is mainly due to densification and swelling. Since the models that represent such fuel deformation are not present in FRAP-T6, FRAPCON-2[18] is used to analyze Rod 32 during the extended low power period up to 12.5 GWd/tUO_2. Then, the modified FRAP-T6 is used for the analysis during a power cycle identical to the one used for Rod 11. Because the initial conditions for the FRAP-T6 analysis are defined by the FRAPCON-2 output, the models for the FRAPCON-2 and FRAP-T6 analyses should be consistent. Both of these models should have the same number of axial and radial nodes with identical coordinates. FRAPCON-2 cannot model the central void along a fraction of the fuel rod length. Therefore, the central void in the upper portion of Rod 32 is not modeled in either the FRAPCON-2 or FRAP-T6 analysis. The radial power profile for high enrichment fuel does not change significantly while increasing burnup.[19] The radial power profile was determined by PNL and used in the FRAPCON-2 and the FRAP-T6 analyses.

The mechanics models[4,5] incorporated in FRAP-T6 during 1982 are not yet incorporated in FRAPCON-2. This discrepancy may affect the FRAPCON-2 calculations of cladding strains and fuel temperatures. However, the impact is expected to be small and can be evaluated after the recently developed mechanics models are incorporated in FRAPCON-2.

In the FRAPCON-2 analysis, cladding creepdown due to a pressure difference (coolant pressure minus the gas pressure) and cladding axial growth due to irradiation take place. These phenomena introduce negative permanent hoop strains and positive permanent axial strains in the cladding. Due to irradiation, the cladding yield strength increases from 140.0 MPa at beginning of life to 400.0 MPa at 12.5 GWd/tUO_2. During the FRAP-T6 analysis, no additional permanent strains are introduced despite the fact that the maximum relative cladding axial strain and hoop strain are as large as those calculated in the analysis of Rod 11. The experimental measurements also confirm that no additional permanent strains are introduced during the power cycle at 12.5 GWd/tUO_2.

Figure 4 shows a comparison of calculated and measured relative cladding extensions for Rod 32 versus fuel rod peak power. The modified FRAP-T6 calculations are shown with the experimental data.[11] The following observations are made:

1. At maximum power, the modified FRAP-T6 calculation of relative cladding extension is 2% greater than the corresponding measurement. At lower powers, the modified FRAP-T6 calculation of relative cladding extension is greater than the corresponding measurements. At 36.0 kW/m, the modified FRAP-T6 calculation is 100% greater than the corresponding measurement. At 47.0 kW/m, the calculation is 58% greater. These discrepancies should be reduced by the proposed implementation scheme for the compliance model discussed in Appendix A.

2. At 36.0 kW/m, the modified FRAP-T6 calculation of the relaxation of cladding extension is 400% greater than the corresponding measurement. This discrepancy may be due to high cladding axial stress caused by the large cladding extension as reported in Observation 2. Therefore, better agreement would be expected if the proposed implementation scheme for the compliance model were used.

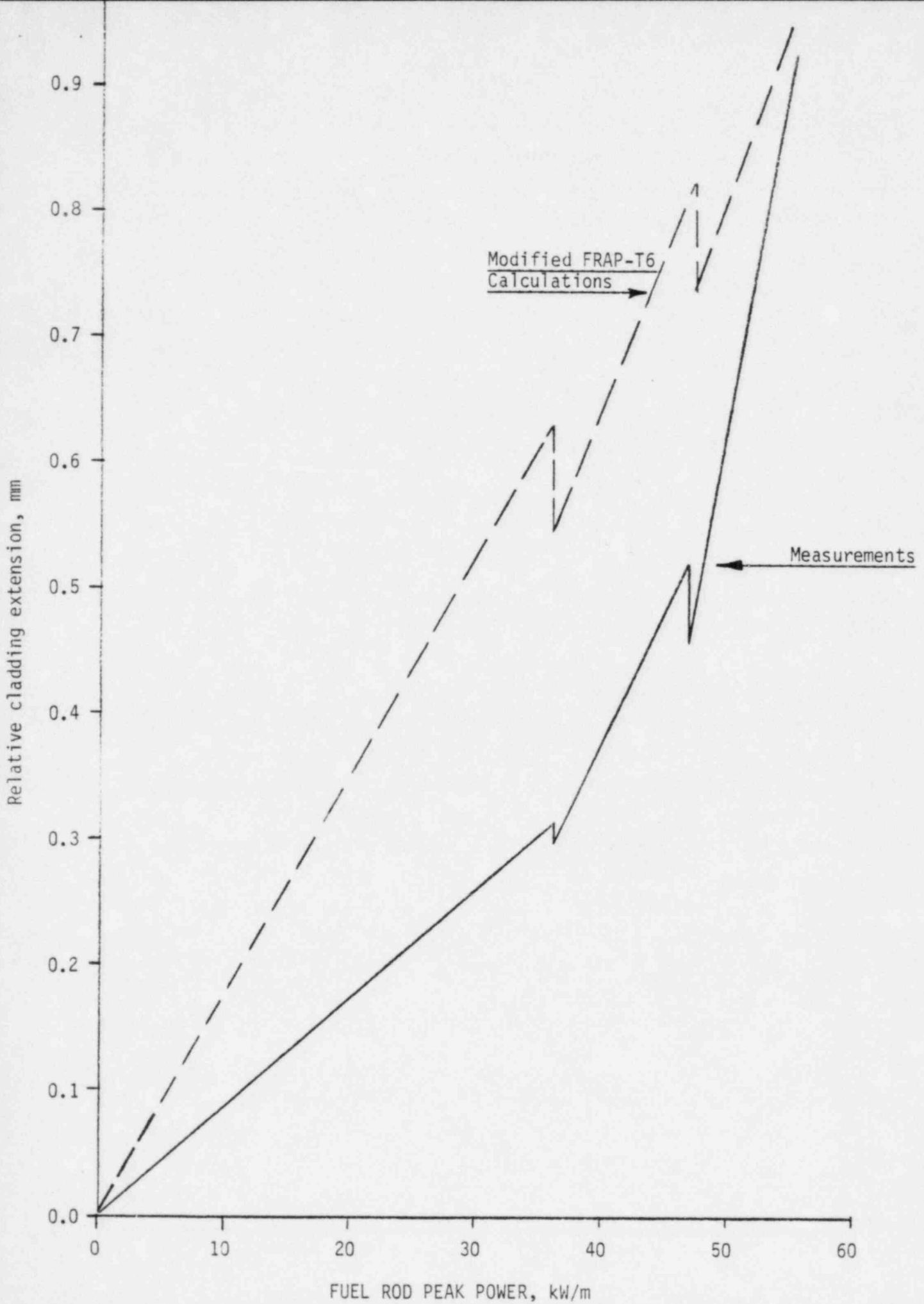

Figure 4. Calculated and measured cladding axial extension versus power for IFA-508 Rod 32 showing the modified FRAP-T6 calculations.

Figure 5 shows the modified FRAP-T6 calculation of cladding hoop strain. The details of the experimental data are not available, but Reference 11 provides information to make qualitative comparisons and is included in the following observations:

1. Comparison of hoop strain measurements from Rod 11 and Rod 32 reveals that the maximum ridge height for Rod 32 was greater than that for Rod 11.[11] This implies that the maximum hoop strain for Rod 32 is greater than that for Rod 11. Comparison of the calculations shows that the maximum hoop strain for Rod 32 is 30% greater than that for Rod 11 (see Figure 3). Therefore, the modified FRAP-T6 calculations for cladding hoop strain are qualitatively correct.

2. The modified FRAP-T6 calculated strain indicates that radial PCMI begins at the beginning of the power cycle, while the measured results show that radial PCMI begins at 20 kW/m.[11]

3. Reference 11 concludes that Rod 32 experienced a small strain reduction during low power holding and a large reduction during high power holding. The modified FRAP-T6 calculations show a large strain reduction during low power holding and a small reduction during high power holding. The modified FRAP-T6 results show an increase in the cladding hoop strain (not shown in Figure 5) when power is held constant at 55 kW/m. These discrepancies in the results imply deficiencies in the fuel creep and fuel relocation relaxation models.[20]

The comparisons presented above indicate that two modifications are needed to improve FRAP-T6 calculations of cladding strain at relatively high fuel burnup. The first modification is concerned with the implementation of the compliance model in FRAP-T6. The approach used to implement this model for the analysis presented in this report required an adjustment in the relocation model which has resulted in the initiation of radial PCMI at the beginning of a power cycle. If the approach proposed in Appendix A were used to implement the compliance model, the observed

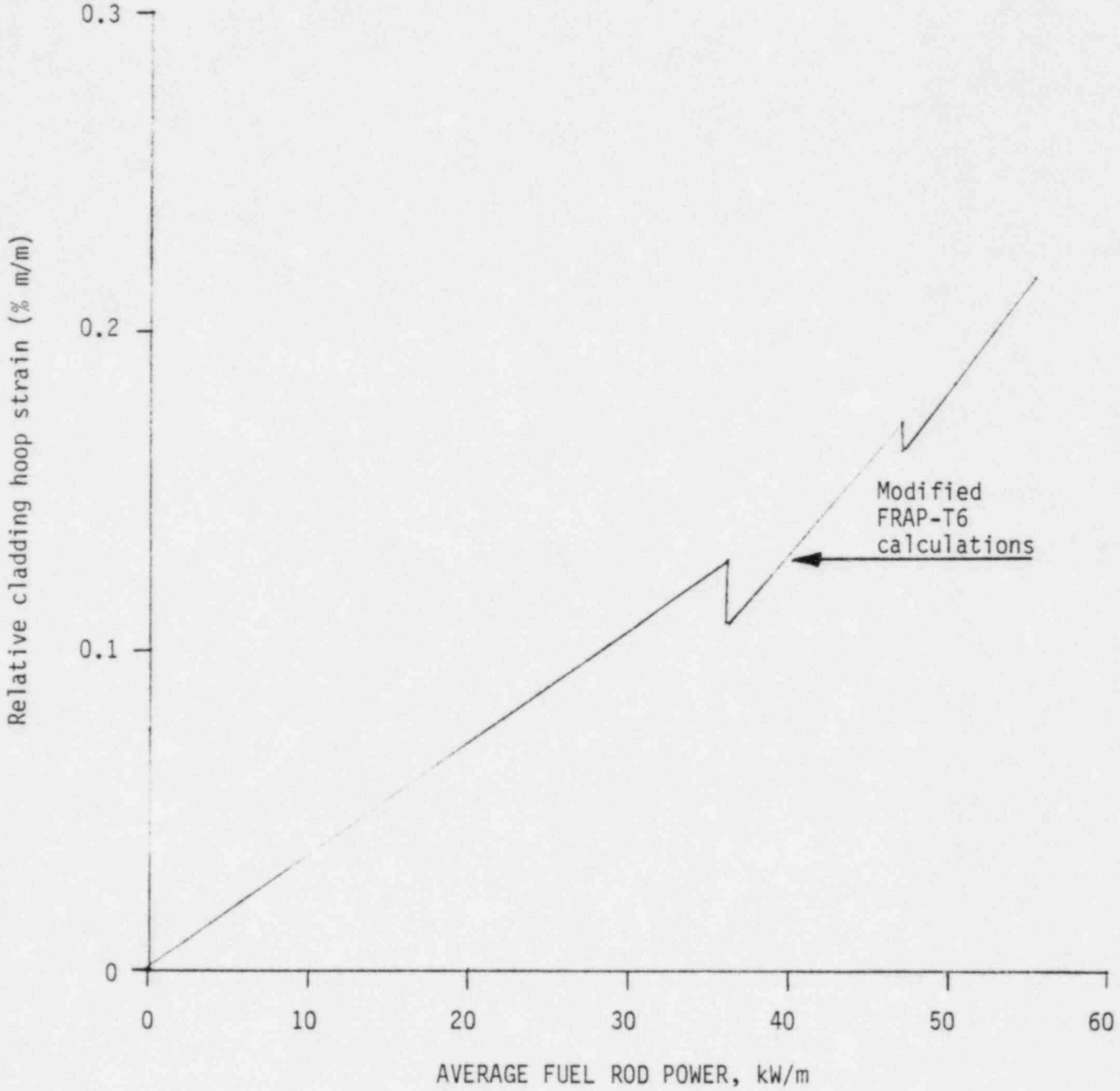

Figure 5. Calculated cladding hoop strains versus power for IFA-508 Rod 32 using the modified FRAP-T6.

discrepancies in cladding strains would be reduced. The second modification is to improve the fuel creep and fuel relocation relaxation models. This modification is further discussed in Section 4.

3.2 IFA-509 Experiment

Comparison of the modified FRAP-T6 calculations and measurements of fuel centerline temperature and cladding diameter change for Rods B1 and B2 of the IFA-509 experiment are presented in this section. Rod B1 has solid fuel pellets, while Rod B2 has hollow fuel pellets. Otherwise, the physical dimensions of Rods B1 and B2 are identical. Fuel in Rod B1 has an enrichment of 10.0 w/o U-235, while fuel in Rod B2 has an enrichment of 10.6 w/o U-235. Otherwise, the material properties for Rods B1 and B2 are identical.[12]

Rods B1 and B2 were irradiated at low power (30 kW/m) to a fuel burnup of 3.0 GWd/tUO_2. Then, these rods were subjected to the power cycle shown in Figure 6. FRAPCON-2 was used to analyze these rods during the low power irradiation, and the modified FRAP-T6 code used to analyze the power history shown in Figure 6.

The FRAPCON-2 code input was modified in order to link FRAPCON-2 and FRAP-T6 when analyzing the hollow fuel pellets (Rod B2). An inconsistency due to the radial node numbering scheme used in these two codes exists when a hole is present in the fuel. In FRAPCON-2, the first radial node is located at the boundary of the hole, while in FRAP-T6 the first radial node is located at the center of the hole. Because of this inconsistency between FRAPCON-2 and FRAP-T6, the fuel pellets in Rod B2 are modeled as solid pellet and the effect of the hole is simulated by manipulating the radial power profile shown in Figure 7. By specifying the radial power to be of small magnitude in the region corresponding to the hole, very little power was generated in this region. Thus, the effect of the central hole in the pellet was simulated.

Figure 8 shows the comparisons of calculated and measured centerline temperatures for Rods B1 and B2 versus average fuel rod power. At maximum

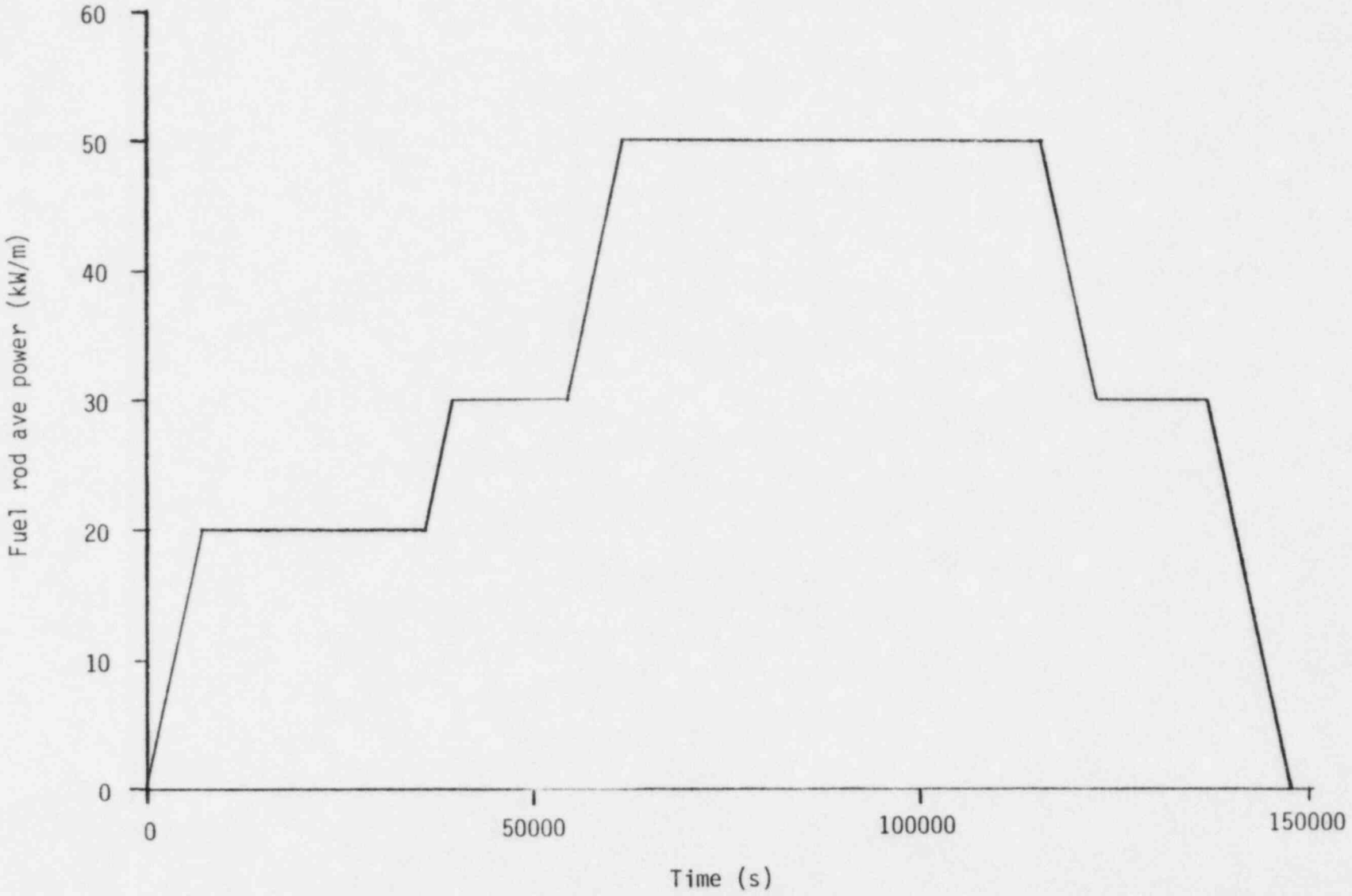

Figure 6. Power cycle used in the modified FRAP-T6 analysis of IFA-509 Rods B1 and B2.

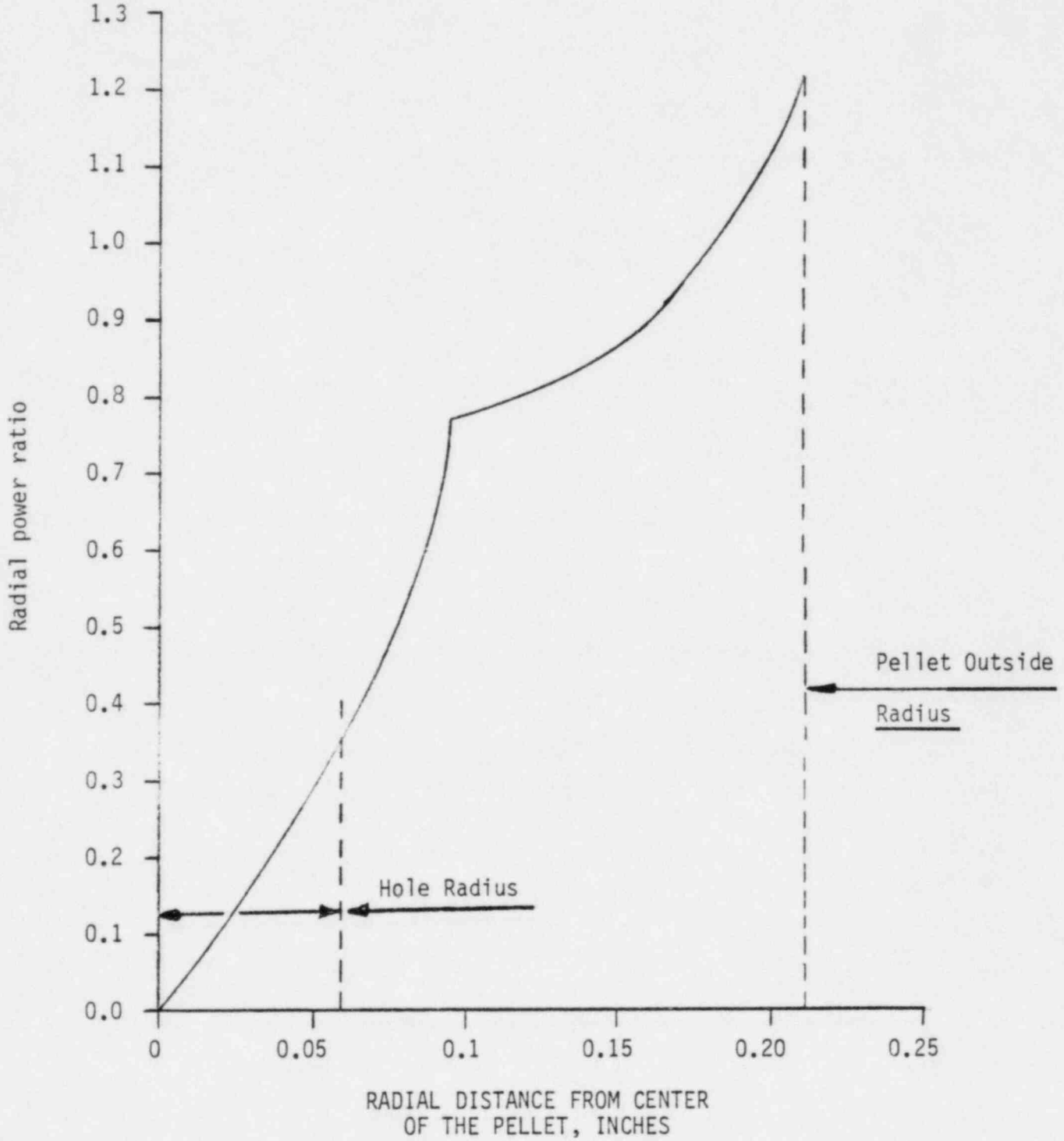

Figure 7. Radial power profile - Rod B2.

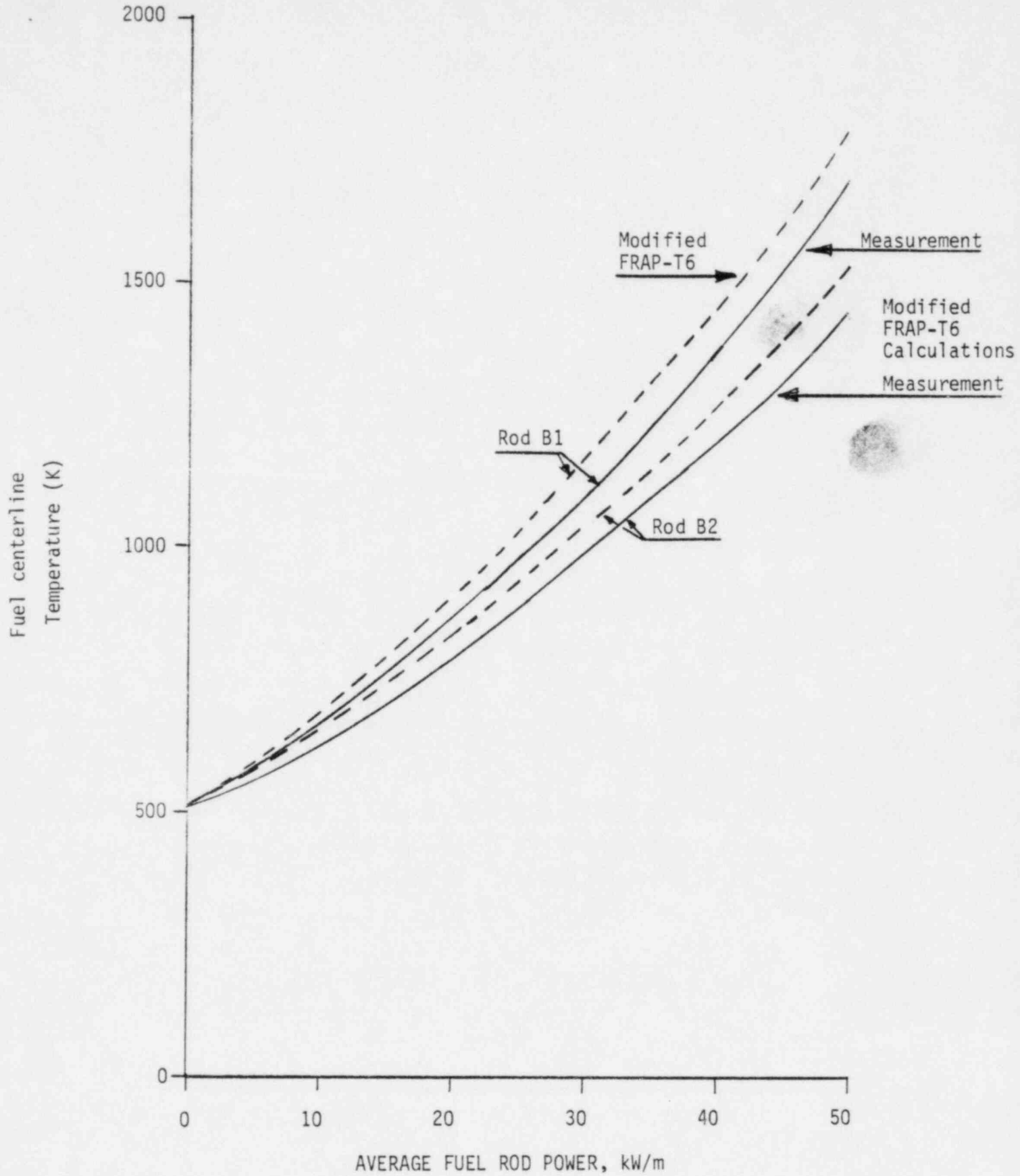

Figure 8. Calculated and measured fuel centerline temperatures versus power for IFA-509 Rods B1 and B2 using the modified FRAP-T6.

power, the calculated temperatures are about 5% greater than the corresponding measured temperatures. These comparisons show that FRAP-T6 accurately calculates centerline temperatures. In addition, comparison of fuel centerline temperatures for Rod B2 shows that a hollow pellet may be modeled by specifying the radial power to be of small magnitude in the region corresponding to the hole (see Figure 7).

Figures 9 and 10 show the comparisons of calculated and measured cladding average diameter changes versus average fuel rod power for Rods B1 and B2. The following observations are made:

1. At maximum power, the modified FRAP-T6 calculations of relative cladding hoop strain in Rods B1 and B2 are 11% and 7% less than the corresponding measurements.

2. The modified FRAP-T6 calculation of the maximum relative cladding hoop strain for Rod B1 (solid pellets) is 13% greater than the corresponding calculation for Rod B2 (hollow pellets). The measurement for the maximum relative cladding hoop strain for Rod B1 is 19% greater than the corresponding measurement for Rod B2.

3. The modified FRAP-T6 calculations show that radial PCMI is initiated at the beginning of the power cycle. The measured cladding hoop strains show that radial PCMI is initiated at 30 and 34 kW/m for Rods B1 and B2, respectively. This discrepancy should be significantly reduced if the compliance model is implemented in FRAP-T6 as presented in Appendix A.

The comparisons presented above indicate that the modified FRAP-T6 calculations of maximum hoop strains are in good agreement with the corresponding measurements. The above comparisons also indicate that the implementation of the compliance model should be modified so that it does not affect the beginning of radial PCMI.

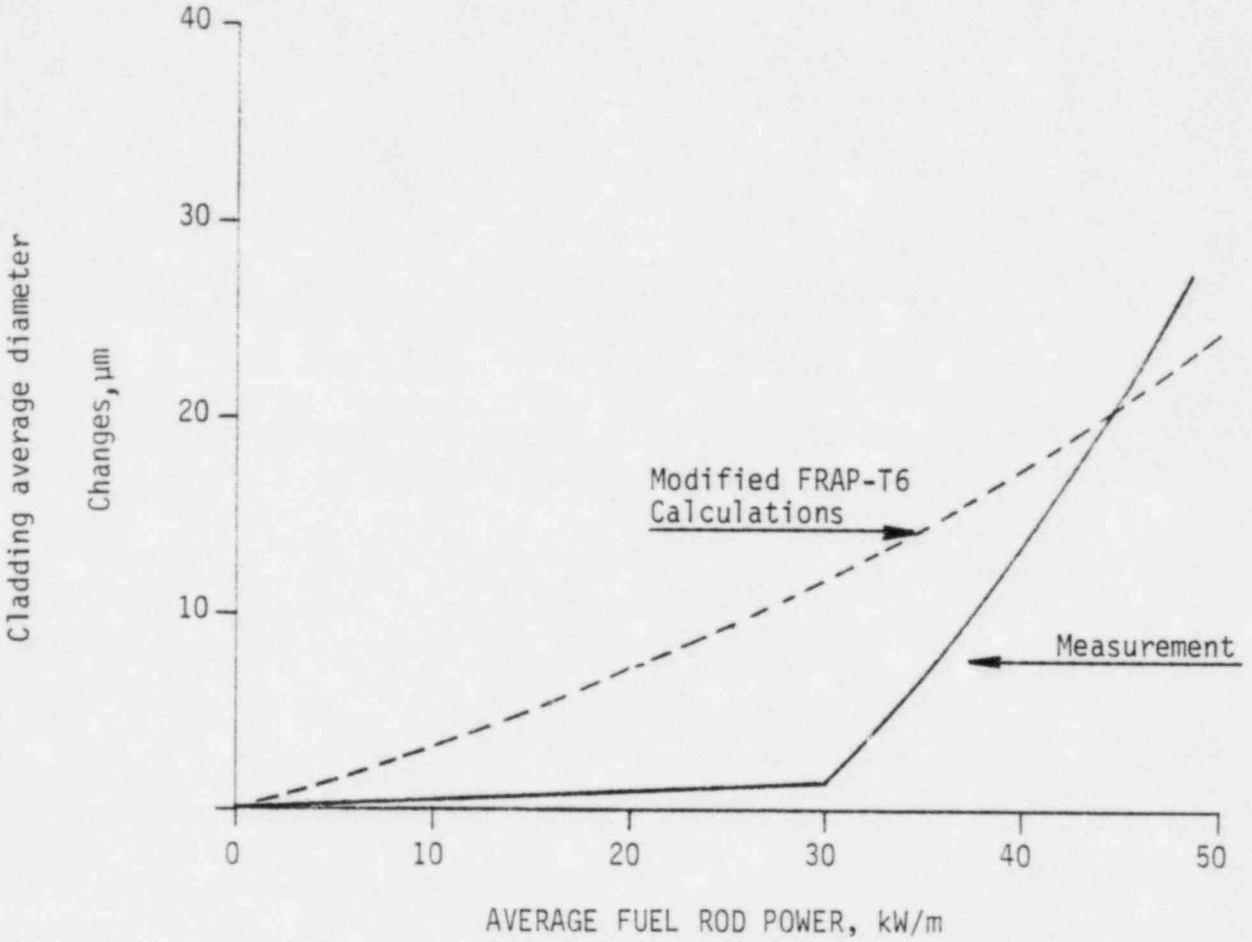

Figure 9. Calculated and measured cladding hoop strains versus power for IFA-509 Rod B1 using the modified FRAP-T6.

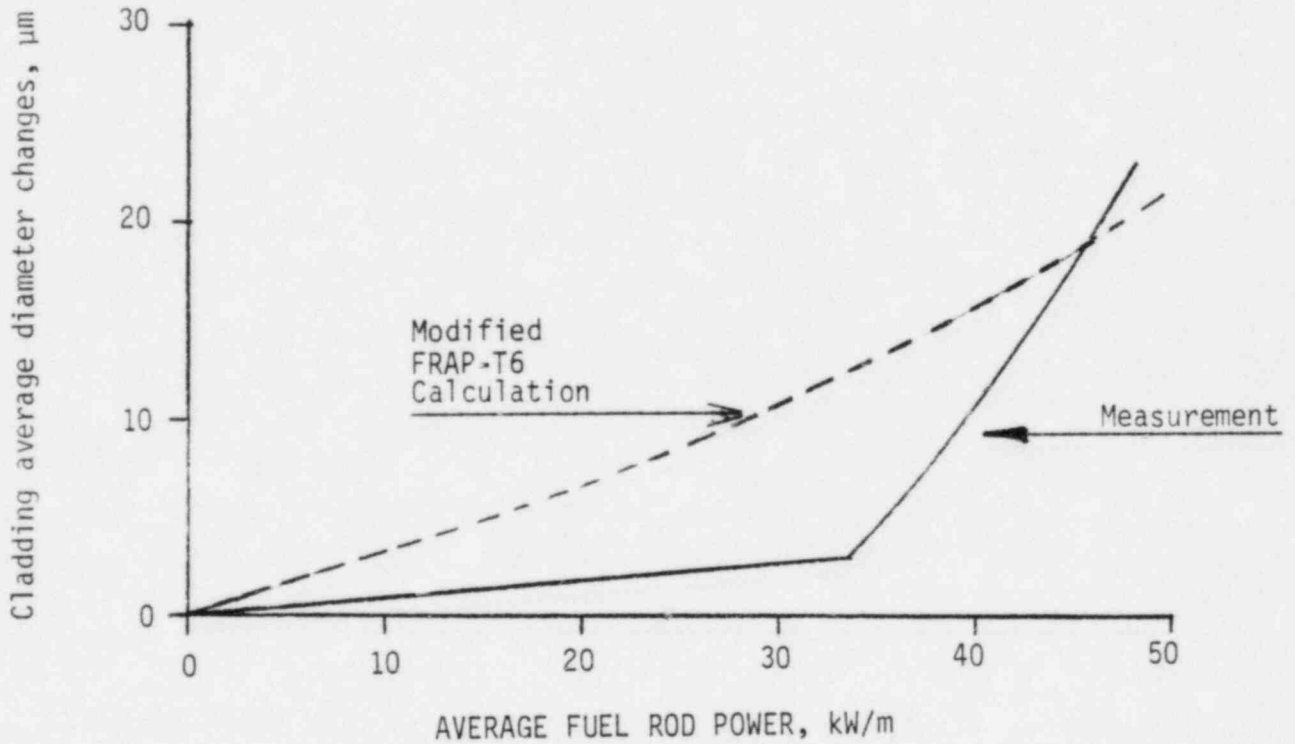

Figure 10. Calculated and measured cladding hoop strains versus power for IFA-509 Rod B2 using the modified FRAP-T6.

3.3 IFA-512 Experiment

Comparisons of the modified FRAP-T6 calculations and the experimental measurements of cladding hoop strains for Rod C in the IFA-512 experiment are presented in this section. Rod C was unpressurized and had radial dimensions typical of BWR fuel. The asfabricated gap size was 102.5 μm. Rod C was irradiated at extended low power (33 kW/m) to a fuel burnup of 10 GWd/tUO_2. Then, it was subjected to the power ramp shown in Figure 11. FRAPCON-2 was used to analyze Rod C during low power irradiation. The modified FRAP-T6 code was used to analyze rod behavior during the power ramp.

Figure 12 shows the comparisons of calculated and measured relative cladding hoop strains versus average fuel rod power. The following observations are made:

1. At maximum power, the modified FRAP-T6 calculation for relative cladding hoop strain in Rod C is 8% less than the corresponding measurement.

2. The modified FRAP-T6 calculation shows that radial PCMI is initiated at 36 kW/m. The measured results show that radial PCMI is initiated at 31 kW/m.

The comparisons presented above indicate that the modified FRAP-T6 calculations for cladding hoop strains compare well with the corresponding measurements.

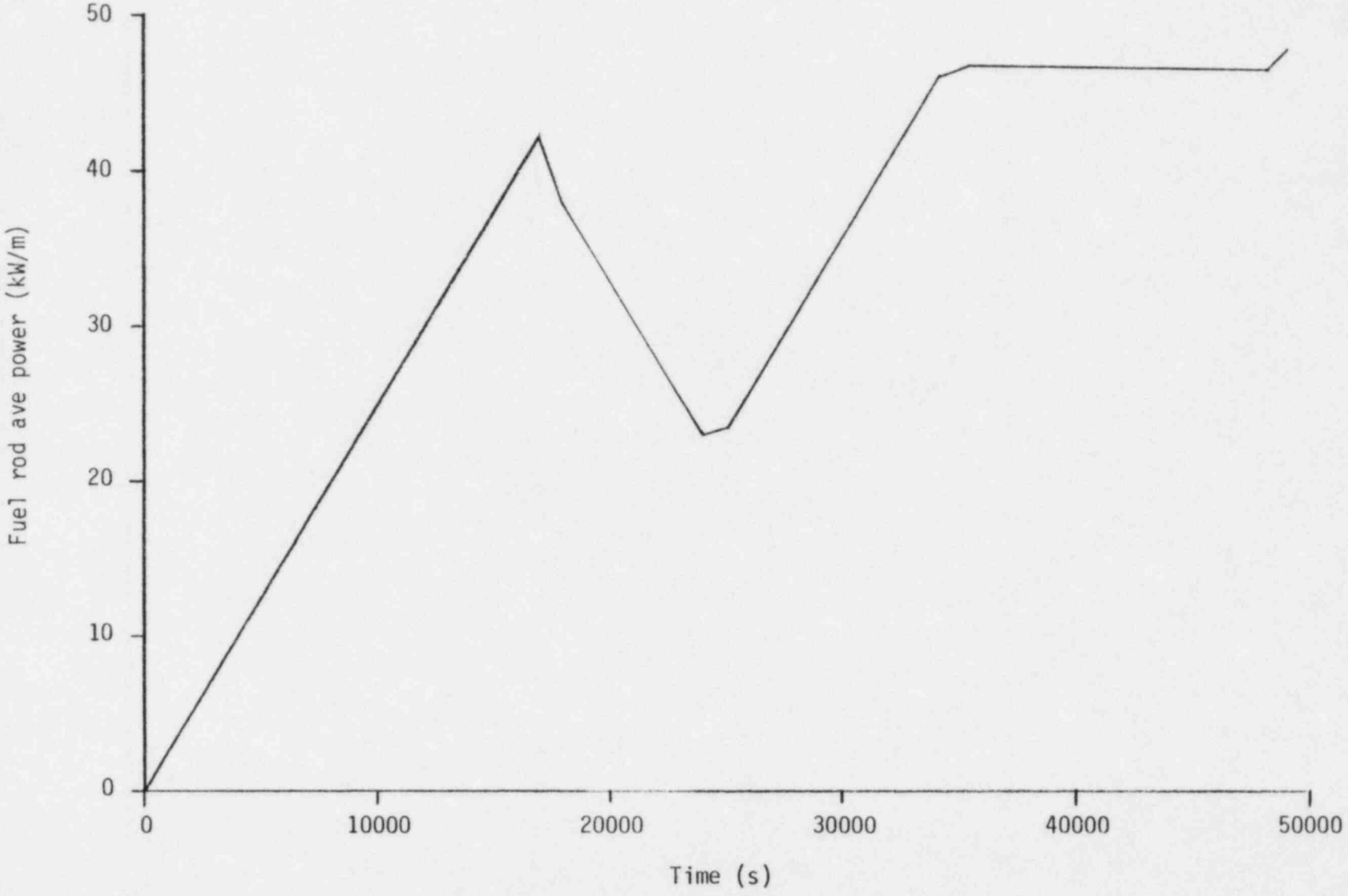

Figure 11. Power ramp used in the modified FRAP-T6 analysis of IFA-512, Rod C1.

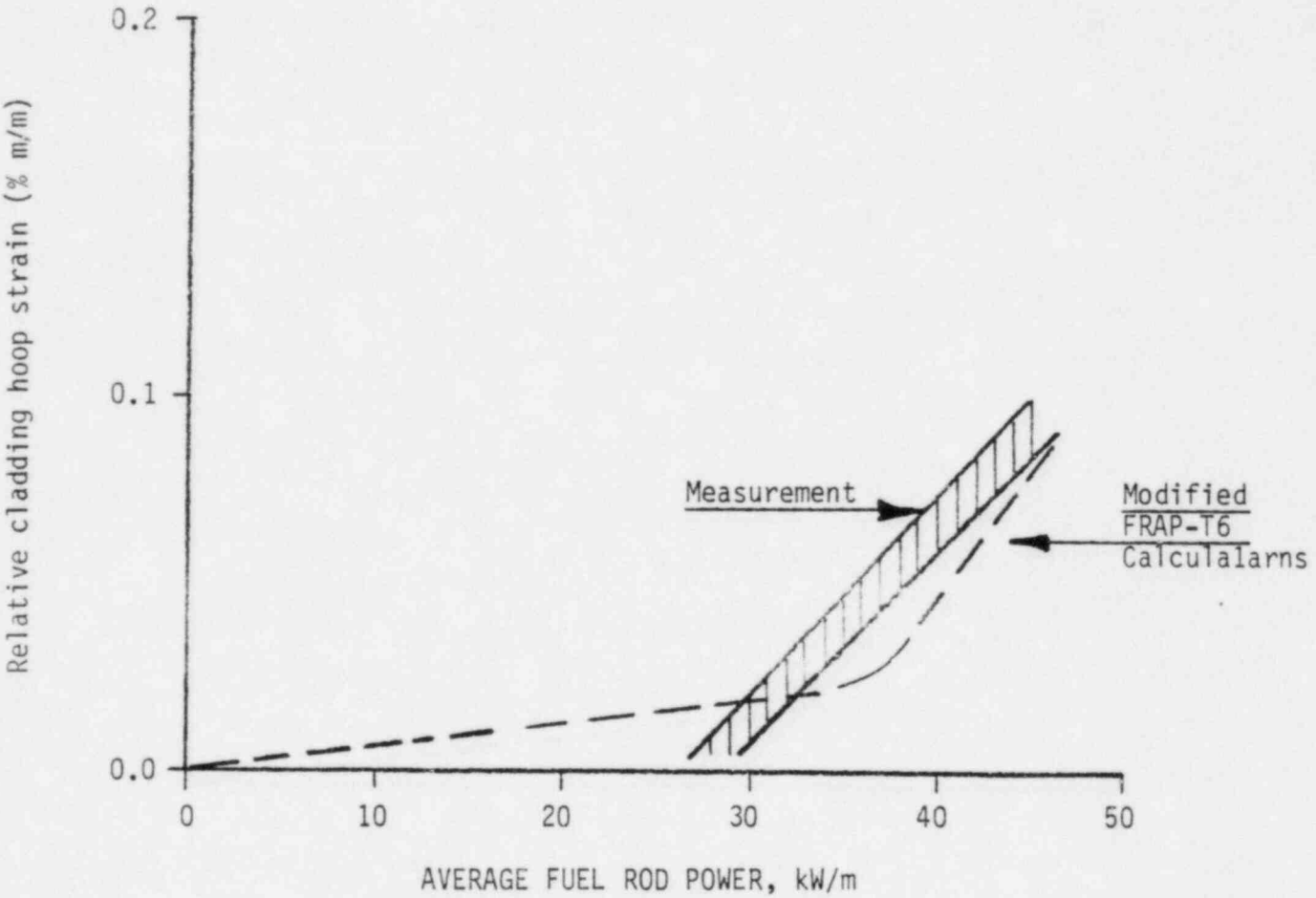

Figure 12. Calculated and measured cladding hoop strains versus power for IFA-512 Rod C using the modified FRAP-T6.

4. CONCLUSIONS AND RECOMMENDATIONS

The comparisons between the modified FRAP-T6 calculations and corresponding experimental data presented in Section 3 demonstrate that the recently developed FRACAS-II models have significantly improved the capabilities of FRAP-T6 to calculate fuel rod mechanical response during conditions of PCMI. This is supported by the comparisons between the calculated and measured cladding axial strains, permanent axial strains, and maximum hoop strains. However, some further improvements are required to complete the PCMI analysis capability. The need for additional modeling improvements and model assessment is justified by the following observations:

1. The compliance model is based on beginning-of-life fuel rod test data (IFA-508, Rod 11). The temporary implementation of this model required adjustment of the relocation and early axial PCMI models which caused initiation of radial PCMI at the beginning of a power cycle for small gap fuel rods with relatively high burnup. This behavior is a typical (see Figures 5, 9, and 10).

2. The calculations of relaxation in cladding axial strains during constant power are signficantly smaller than the corresponding test results (see Figure 2). Some calculations of relaxation in cladding hoop strain are significantly less than the corresponding test results (see Figure 3). Some calculations even show negative relaxation in cladding hoop strain (see Figure 3 and Observation 1 for Rod 32). The relaxation in the cladding strains is due to fuel creep and fuel relocation relaxation. Therefore, the discrepancies in the relaxation of cladding strains is due to deficiencies in the fuel creep and fuel relocation relaxation models.

3. The cladding yield strength and ultimate strength models in FRAP-T6 predict significantly higher strengths for the cladding material used in the Halden experiments (see Table 1).

4. The fuel compliance model, relocation relaxation model, and the effective fuel thermal expansion model are based on only the beginning-of-life data from the IFA-508, Rod 11 experiment.

The above observations indicate that the major deficiencies in the structural models of FRAP-T6 are associated with the constitutive models. Based on these observations, several modifications and further evaluation efforts have been formulated which, if performed, should result in calculations of uniform cladding axial stress and maximum cladding hoop stress which will be sufficiently accurate to perform SCC analysis and to determine cladding failure probability. The specific recommendations are listed below.

1. The compliance model presented in this report has significantly improved the cladding hoop strain calculations for IFA-508 Rod 11 at beginning-of-life. The implementation scheme for the compliance model used in the analysis presented in this report is such that the initiation of radial PCMI is calculated to occur at the beginning of power cycles for fuel rods with relatively high burnup (see Figures 5, 9 and 10). It is recommended that the implementation scheme for the compliance model proposed in Appendix A be adopted. This scheme would result in the calculation of the initiation of radial PCMI at power levels shown by the experimental data for fuel rods at relatively high burnup and in more accurate calculations of maximum cladding hoop strains.

2. The fuel creep model in FRAP-T6 needs to be replaced. This model calculates stress by taking into account only two parameters: the fuel temperature and strain rate. It is based on outdated experimental creep down data.[21] A candidate replacement model is the MATPRO fuel creep model, FCREEP.[7]

FCREEP models creep strain rate as a function of time, temperature, grain size, density, fission rate, oxygen-to-metal ratio, and external stress.

3. The implementations of the fuel creep model and the fuel relocation relaxation model in FRAP-T6 are not consistent. The fuel creep model is implemented using Prandtl-Reuss equations while the implmentation of the fuel relocation relaxation model is rather arbitrary. It is recommended that the yield function developed by Rashid[20] and the associated flow rule be used to implement these two fuel deformation models. Fuel creep would then be a function of deviatoric stress and, therefore, will present a constant volume creep. Fuel relocation relaxation would be a function of hydrostatic stress and, therefore, will represent a non-constant volume creep. It should be noted that this yield function has been successfully used in other fuel rod performance analysis codes, i.e., FREY[22] and FEMAXI.[23]

4. The materials models in FRAP-T6 significantly overpredict cladding stengths for fuel rods used in the Halden reactor and commercial reactors. FRAP-T6 overpredicts yield and ultimate strengths of tha cladding used in the beginning-of-life experiments at Halden. This deficiency has resulted in significant error in the calculation of cladding permanent strains and in clading stresses. It is recommended that the models in MATPRO be reviewed and updated as appropriate.

5. The fuel compliance model, relocation relaxation model, and the effective fuel thermal expansion model are based on beginning-of-life data from the IFA-508, Rod 11 experiment. FRAP-T6 analyses and a literature survey[10,24] have shown that this data base is inadequate and that more evaluation of these models is needed. It is recommended that a broader data base be used to refine these models. Most of the required data may come from selected Halden and PBF experiments. The experiments should be selected so that the data represent the effects of the

following parameters on cladding stresses and strains: asfabriacted gap size, pellet design parameters, burnup levels, steady state and transient power cycles, cladding materials properties, and fuel materials properties.

The above recommendations, if incorporated in FRAP-T6, will correct the known modelling defficiencies and should improve the calculations of cladding stresses and strains to a degree acceptable for reliably determining fuel rod failure probabilties for commercial rods due to PCMI-SCC provided a model is developed and incorporated in FRAP-T6 to calculate localized axial stresses. It is recommended that an empirical model be developed for this purpose after the above mentioned modeling improvements are completed. The model can be developed using computer codes designed for detailed local cladding stress analyses i.e., FEMAXI, FREY, or AXISYM.

5. REFERENCES

1. L. J. Siefken, Developmental Assessment of FRAP-T6, EGG-CDAP-5439, May 1981.

2. R. Chambers et al., Independent Assessment of the Transient Fuel Rod Analysis Code FRAP-T6, EGG-CAAD-5532, August 1982.

3. M P. Bohn, FRACAS-II: A Subcode for the Mechanical Analysis of Nuclear Fuel Rods, CADP-TR-78-038, September 1978.

4. V. N. Shah and G. A. Berna, Constitutive Models for the FRACAS-II Subcode of FRAP-T6, EGG-NSMD-6103, November 1982.

5. V. N. Shah, E. R. Carlson, and G. A. Berna, "Advanced Deformation Models for FRAP-T6," EGG-CDAP-6054, September 1982.

6. J. Rest, GRASS-SST: A Comprehensive Mechanistic Model for the Prediction of Fission Gas Behavior in UO_2 Based Fuels During Steady State and Transient Conditions, NUREG/CR-0202, ANL-78-53, June 1978.

7. D. L. Hagrman (ed.) MATPRO--Version 11 (Revision 1): A Handbook of Material Properties for Use in the Analysis of Light Water Reactor Fuel Rod Behavior, NUREG/CR-0497, TREE-1280, Rev. 1, February 1980.

8. L. J. Siefken, Moaidficaiton of Stress Corrosion Cracking Model in FRAP-T6, CDF-FT-32, November 1982.

9. E. R. Calrson, A Model for Fuel Rod Gap Gas Release to Coolant, EGG-CDD-5817, March 1982.

10. S. Aas, Mechanical Interaction Between Fuel and Cladding, Nuclear Engineering and Design, 21, 1972, pp. 237-253.

11. K. Yanagisawa, In Reactor Measurements of the Influence of Extended Low Power Prior to Power Increases, Enlarged Halden Programme Group Meeting on Water Reactor Fuel Performance and Application of Process Computers in Reactor Operation, HPR-267, June 1980.

12. D. Zorini, E. Kolstad, and H. V. Staal, Preliminary Analysis of Deformation Characterization in Solid and Hollow Fuel Pellet Rods During Ramp Operation in the 3-Rod Diameter Rig IFA-509-2, HWR-19, 1981.

13. G. L. Hunt, USNRC HALDEN DELEGATE MONTHLY REPORT, August 1982.

14. Enlarged Halden Programme Group Meeting on Fuel Experiments and Performance Analysis, June 13-18, 1982. (Held in conjunction with the seventy-fourth meeting of the Halden Programme Group).

15. K. Ito, Y. Wakashima and M. Oguma, "Pellet Compliance Model Based on Out-of-Pile Simulation," Nuclear Engineering and Design, 56, pp. 117-122, 1980.

16. V. N. Shah, Developmental Assessment of FRACAS-II, EGG-CDAP-5411, p. 25, May 1981.

17. S. A. Ploger and T. F. Cook Postirradiation Examination Results for the Irradiation Effects Test IE-3, TREE-NUREG-1200, March 1978, p. 123.

18. G. A. Berna et al., FRAPCON-2: A Computer Code for the Calculation of Steady State Thermal-Mechanical Behavior of Oxide Fuel Rods, NUREG/CR-1845, December 1980.

19. Private Communications with D. D. Lanning, PNL, Richland, Washington.

20. Y. R. Rashid, et al., Mathematical Treatment of Hot Pressing of Reactor Fuel, Nuclear Engineering and Design, 29, pp. 1-6, 1974.

21. P. E. Bohaboy et al., Compressive Creep Characteristics of Staichiometric Uranium Dioxide, GEAP-10054, May 1969.

22. Private Communications with Professor M. N. Sharabi, San Diego State University, San Diego, California.

23. M. Ichikawa, et al., FEMAXI-III: An Axisymmetric Finite Element computer code for the Analysis of Fuel Rod Performance, IAEA Specialists Meeting on Water Reactor Fuel Element Performance Computer Modeling, Blackpool, UK, March 1980.

24. K. O. Vilpponen et al., Mechanical Behavior of Fuel Rods at High Burnup, Enlarged Halden Programme Group Meeting, June 1978.

APPENDIX A

PROPOSED SCHEME FOR IMPLEMENTATION OF FUEL COMPLIANCE MODEL

The FRACAS-II subcode precisely calculates the instant when axial PCMI begins but does not perform a similar calculation for the beginning of radial PCMI. To implement the fuel compliance model described in Section 2, the first modification would be to determine the radial displacement of the fuel outer surface, URF_o, at the beginning of radial PCMI. This modification would replace Equation (1). Also, Equation (2) would be replaced by the following equation in TRANSF:

$$URC = URF_o + (URF - URF_o)\ COMPF - DELTA \quad . \qquad (A\text{-}1)$$

The proposed implementation does not require any additional changes in the fuel relocation model or any change in the locking gap parameter. It should be noted that this modified implementation is similar to the one used to model effective thermal expansion of fuel. (Effective fuel thermal expansion model was called fuel-cladding axial slippage model in Reference 4).